© 2014. Published by The Company of Biologists Ltd | Development (2014) 141, 3388-3398 doi:10.1242/dev.106005

RESEARCH ARTICLE

Nuclear removal during terminal lens fiber cell differentiation requires CDK1 activity: appropriating mitosis-related nuclear disassembly

Blake R. Chaffee[1], Fu Shang[2], Min-Lee Chang[2], Tracy M. Clement[3], Edward M. Eddy[3], Brad D. Wagner[1], Masaki Nakahara[4], Shigekazu Nagata[5], Michael L. Robinson[1,*] and Allen Taylor[2,6,*]

ABSTRACT

Lens epithelial cells and early lens fiber cells contain the typical complement of intracellular organelles. However, as lens fiber cells mature they must destroy their organelles, including nuclei, in a process that has remained enigmatic for over a century, but which is crucial for the formation of the organelle-free zone in the center of the lens that assures clarity and function to transmit light. Nuclear degradation in lens fiber cells requires the nuclease DNase IIβ (DLAD) but the mechanism by which DLAD gains access to nuclear DNA remains unknown. In eukaryotic cells, cyclin-dependent kinase 1 (CDK1), in combination with either activator cyclins A or B, stimulates mitotic entry, in part, by phosphorylating the nuclear lamin proteins leading to the disassembly of the nuclear lamina and subsequent nuclear envelope breakdown. Although most post-mitotic cells lack CDK1 and cyclins, lens fiber cells maintain these proteins. Here, we show that loss of CDK1 from the lens inhibited the phosphorylation of nuclear lamins A and C, prevented the entry of DLAD into the nucleus, and resulted in abnormal retention of nuclei. In the presence of CDK1, a single focus of the phosphonuclear mitotic apparatus is observed, but it is not focused in CDK1-deficient lenses. CDK1 deficiency inhibited mitosis, but did not prevent DNA replication, resulting in an overall reduction of lens epithelial cells, with the remaining cells possessing an abnormally large nucleus. These observations suggest that CDK1-dependent phosphorylations required for the initiation of nuclear membrane disassembly during mitosis are adapted for removal of nuclei during fiber cell differentiation.

KEY WORDS: CDK1, Lens fiber differentiation, Organelle-free zone, Mouse

INTRODUCTION

The ocular lens and cornea are the only clear tissues in the body. Opacification of the normally clear lens (called a cataract), afflicts 80% of the elderly population and remains the most common cause of blindness worldwide, afflicting over 19 million people (WHO, 1998; http://www.who.int/whr/1998/en/). As such, cataracts contribute significantly to the $139 billion spent annually in the USA alone due to compromised vision (http://preventblindness.org/significant-increase-costs-vision-related-diseases).

Mammalian lenses develop from a surface ectoderm-derived vesicle. The anterior cells of the vesicle differentiate into lens epithelial cells, while the cells that make up the posterior half of the vesicle differentiate into primary fiber cells. A single layer of epithelial cells lines the anterior hemisphere of the lens. Although, initially, all lens epithelial cells proliferate, only a band of epithelial cells slightly anterior to the lens equator undergoes cell division in the mature lens. Posterior to this zone, the epithelial cells begin to differentiate to form secondary fiber cells. These fibers elongate and eventually form the bulk of lens tissue. The lens continues to grow throughout life, such that the original fibers, or oldest cells, occupy the lens center with progressively younger fiber cells found closer to the lens surface. Proper differentiation of fiber cells also involves formation of an organelle-free zone (OFZ) comprising fiber cells from which light-scattering intracellular organelles, including the cell nucleus, are removed (reviewed by Wride, 2011). Failure to form the OFZ results in a cataractous lens. Although denucleation was observed more than a century ago (Rabl, 1899), the molecular mechanisms leading to lens fiber cell denucleation remain poorly understood.

The lysosomal nuclease DNase IIβ (DLAD) is essential for breaking down lens fiber cell DNA and establishing an OFZ and clear lens (Nishimoto et al., 2003; De Maria and Bassnett, 2007; Nakahara et al., 2007). Lysosomal/cytoplasmic DLAD gains access to and destroys chromatin DNA upon disassembly of the nuclear membrane (Bassnett and Mataic, 1997). This is reminiscent of mitosis. In proliferating cells, mitosis requires cyclin-dependent kinase 1 (CDK1) in conjunction with cyclins A or B to phosphorylate nuclear membrane lamins to destabilize the nuclear envelope (reviewed by Nigg, 1993). Activated CDK1 also aids in regulating mitotic chromatin (reviewed by Nigg, 1993; Kotak et al., 2013; Orthwein et al., 2014; Zheng et al., 2014). By contrast, post-mitotic cells rarely exhibit CDK1 and cyclin A/B expression (King et al., 1994; Tommasi and Pfeifer, 1995). However, post-mitotic lens fiber cells contain both CDK1 and cyclin B protein (He et al., 1998), suggesting that these proteins might initiate nuclear envelope disassembly to provide access for DLAD during terminal differentiation.

The CDK inhibitors $p57^{KIP2}$ and $p27^{KIP1}$ also regulate CDK1 and the G1/S transition-regulating kinase CDK4 (Sherr and Roberts, 1999). Increased synthesis of $p57^{KIP2}$ and $p27^{KIP1}$ characterizes the withdrawal from the cell cycle and the initiation of lens fiber cell differentiation (Zhang et al., 1997, 1998; Lovicu and McAvoy, 1999; Nagahama et al., 2001; Reza et al., 2007). As differentiation progresses, fiber cells continue to elaborate crystallins: the major fiber cell gene products.

[1]Department of Biology, Miami University, Oxford, OH 45056, USA. [2]Laboratory for Nutrition and Vision Research, Human Nutrition Research Center on Aging, Nutrition &Vision Res-USDA-HNRCA, Tufts University, Boston 02111, MA, USA. [3]National Institute of Environmental Health Sciences, NIH, Research Triangle Park, NC 27709, USA. [4]Department of Molecular and Cellular Physiology, Graduate School of Medicine, Kyoto University, Kyoto, Japan. [5]Department of Medical Chemistry, Graduate School of Medicine, Kyoto University, Kyoto, Japan. [6]Department of Biological Chemistry, Weizmann Institute of Science, Rehovot, Israel.

*Authors for correspondence (robinsm5@miamioh.edu; allen.taylor@tufts.edu)

Received 12 November 2013; Accepted 7 July 2014

Development (2014) 141, 3388-3398 doi:10.1242/dev.106005

Several lines of evidence suggest that a ubiquitin proteasome system participates in nuclear breakdown. First, poly-ubiquitylated conjugates increase in equatorial epithelial cell nuclei just prior to fiber cell differentiation, and localize to differentiating fiber cell nuclei (Shang et al., 1999). Second, zebrafish containing a mutation in the 26S proteasome gene *Psmd6* experience abnormal retention of fiber cell nuclei, as well as a number of cell cycle alterations in the lens epithelium (Imai et al., 2010). Proteosomal degradation of cyclins A and B during mitosis inactivates CDK1, facilitating reformation of the nuclear membrane in daughter cells subsequent to karyokinesis. Cyclins A and B re-accumulate during the G2 phase of the cell cycle to activate CDK1 in preparation for the next mitosis. However, transgenic mice expressing a mutated ubiquitin (K6W-Ubiquitin) in the lens fiber cells accumulated $p27^{KIP1}$, decreased phosphorylation of nuclear lamins A and C, retained nuclei within the usual OFZ, delayed synthesis of crystallins, and were cataractous (Caceres et al., 2010). Together, these data suggested that CDK1 is prominent in directing lens fiber cell denucleation.

Here, we tested the hypothesis that, as in mitotic cells, the disassembly of the nuclear envelope in terminally differentiating fiber cells requires CDK1. We suggest that, in contrast with cycling cells, where CDK activators and inhibitors are cyclically regulated, in lens fibers there is a unidirectional pathway in which high levels of $p57^{KIP2}$ and $p27^{KIP1}$ keep CDK1 inactive in immature fiber cells. However, prior to the formation of the OFZ, diminishing levels of these CDK inhibitors lead to CDK1 activation, lamin phosphorylation, disassembly of the nuclear membrane, entry of DLAD, reorganization of chromatin and destruction of the nucleus. Deletion of *Cdk1* from the lens lineage facilitated the testing of this hypothesis.

RESULTS

CDK1 protein expression in epithelial cells and differentiating lens fibers

Although previous studies have documented the presence of CDK1 protein in lens fiber cells (He et al., 1998), the subcellular localization of CDK1 remained unknown. As expected, the lens epithelium expressed abundant CDK1 and much of the enzyme appeared to be localized to nuclei in epithelial and outer cortical fiber cells (Fig. 1, zones 1, 2). In secondary lens fiber cells, the overall level of CDK1 expression declined as development advanced (compare right with left side, lower panels). Although CDK1 was obvious in both the cytoplasm and nuclei of elongating cells (Fig. 1, zone 2), it remained most concentrated in the nuclei of the deeper fiber cells (Fig. 1, zones 3, 4).

Removal of CDK1 from the lens

Transgenic mice homozygous for the loxP-flanked (floxed) allele of *Cdk1* and hemizygous for the *MLR10* Cre transgene (*MLR10; $Cdk1^{L/L}$*) were created to remove CDK1 from the lens. Cre expression in *MLR10* transgenic mice initiates at E10.5 and this transgene can effectively delete loxP-flanked alleles in both lens epithelial cells and lens fiber cells (Zhao et al., 2004). In the *MLR10; $Cdk1^{L/L}$* lenses, the overall expression of CDK1 protein became mosaic by E15.5 (supplementary material Fig. S1D-F) with few CDK1-positive epithelial cells remaining by E17.5 (Fig. 2B,D, white arrows). By comparison with expression in lens, *MLR10; $Cdk1^{L/L}$* retinas displayed no alterations in CDK1 expression relative to control littermates (Fig. 2E, supplementary material Fig. S1F), indicating that the Cre transgene properly targeted the lens without affecting other tissues within the optic cup. CDK1 protein persisted in postnatal epithelial cells and fiber cells from both control lenses.

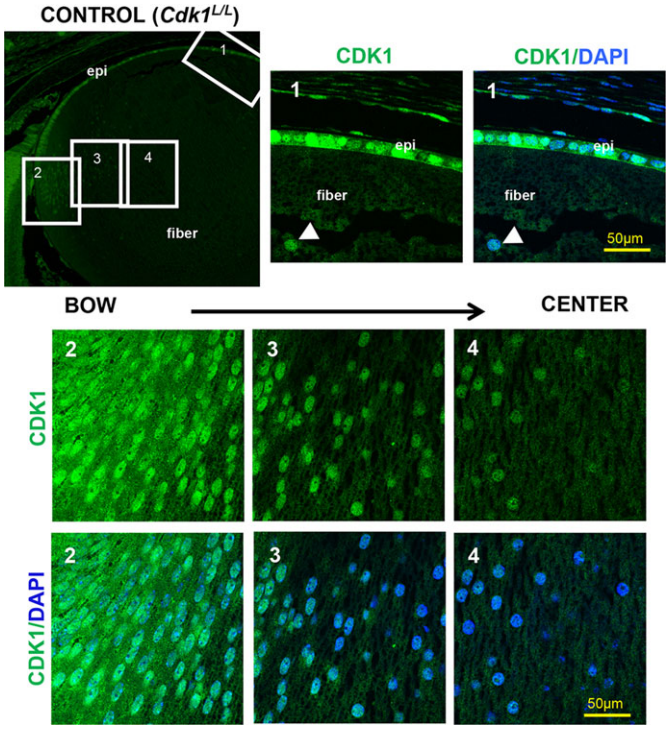

Fig. 1. CDK1 protein expression in normal lens epithelial cells and fiber cells. Anti-CDK1 antibodies detected CDK1 protein in control (Cre negative) mice where the floxed *Cdk1* allele (*$Cdk1^{L/L}$*) remained intact. Zones of the E17.5 lens were subdivided into central epithelium (1) and fiber cells (2-4), with higher numbers representing progressively older fiber cells. These zones (depicted in the upper left panel) are shown at higher magnification with (CDK1/DAPI) and without (CDK1) nuclear counterstaining with DAPI. Although CDK1 protein appeared in both the cytoplasm and nucleus of epithelial cells, and in fiber cells of the bow region (regions 1 and 2), CDK1 protein exclusively localized to the nucleus of deeper (older) fiber cells (left side of arrowheads in region 1, regions 3 and 4). epi, lens epithelium; fiber, lens fiber cells. Scale bars: 50 μm.

Western blots corroborated the diminution of CDK1 at E18.5 in *MLR10; $Cdk1^{L/L}$* lenses (Fig. 2F). The remaining protein indicates that some epithelial cells escape Cre-mediated deletion or, alternatively, represents persistent CDK1 protein produced from transcripts that existed prior to the deletion of *Cdk1*.

To isolate *Cdk1* deletion to lens fiber cells, *MLR39* transgenic mice were bred to *$Cdk1^{L/L}$* animals to generate *MLR39; $Cdk1^{L/L}$* mice. Cre expression in *MLR39* mice initiates at embryonic day 12.5 (E12.5) and, within the lens, remains exclusively in the fiber cell compartment (Zhao et al., 2004). Immunohistochemical and western blot comparisons between the lenses from *MLR39; $Cdk1^{L/L}$* mice and those of Cre negative control littermates (*$Cdk1^{L/L}$*) failed to reveal significant diminution of CDK1 in fiber cells from the P0 *MLR39; $Cdk1^{L/L}$* mice (supplementary material Fig. S1A-C,G). In addition, *MLR39; $Cdk1^{L/L}$* lenses remained clear and appeared histologically identical to control lenses (data not shown). The persistence of CDK1 protein in the lens fibers indicated that the *MLR39* transgene failed to delete the *Cdk1* gene early enough to significantly reduce CDK1 protein in the fiber cell compartment. Therefore, all subsequent analyses employed *MLR10; $Cdk1^{L/L}$* mice.

Loss of CDK1 delays denucleation of lens fiber cells

The gross morphology of *MLR10; $Cdk1^{L/L}$* lenses appeared similar to control lenses at E12.5, prior to fiber cell denucleation, (Fig. 3A,B). However, by E15.5, the nuclei in the differentiating secondary fibers

Development (2014) 141, 3388-3398 doi:10.1242/dev.106005

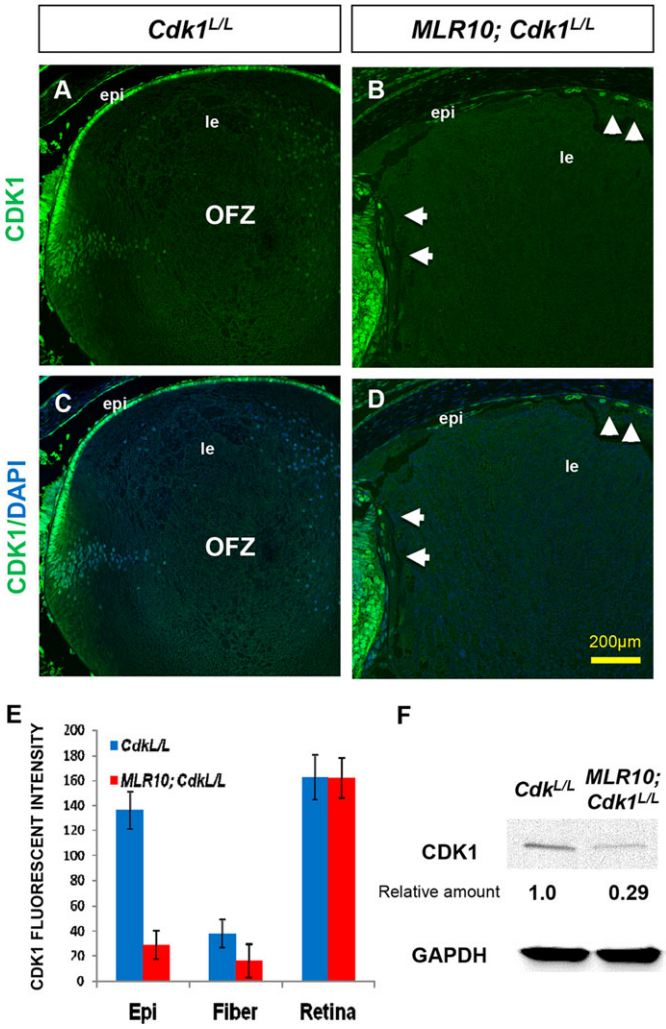

Fig. 2. Little CDK1 expression remains in *MLR10; Cdk1$^{L/L}$* lens cells by E17.5. (A-D) *Cdk1$^{L/L}$* (A,C) and *MLR10; Cdk1$^{L/L}$* (B,D) lenses were compared at E17.5 for the expression of CDK1 with (C,D) and without (A,B) nuclear counterstaining with DAPI. (A,C) Abundant CDK1 was detected throughout the entire epithelium (epi) and in early differentiating fiber cell nuclei of *Cdk1$^{L/L}$* lenses. (B,D) By contrast, CDK1 was absent from most of the *MLR10; Cdk1$^{L/L}$* lens epithelium and only a few CDK1-positive nuclei are observed in early differentiating fiber cells (arrows). (E) Relative CDK1 levels were estimated via immunofluorescent intensity measurements. CDK1 protein levels were similar in the retinas of Cdk1$^{L/L}$ and *MLR10; Cdk1$^{L/L}$* mice. le, lens; OFZ, organelle-free zone. Data are the mean ± s.e.m., with each bar representing 12 measurements (four different embryos with three sections each). (F) Western blotting of total lens protein from E18.5 lenses revealed a marked reduction in CDK1 in *MLR10; Cdk1$^{L/L}$* lenses with GAPDH as a loading control. Scale bars: 200 μm.

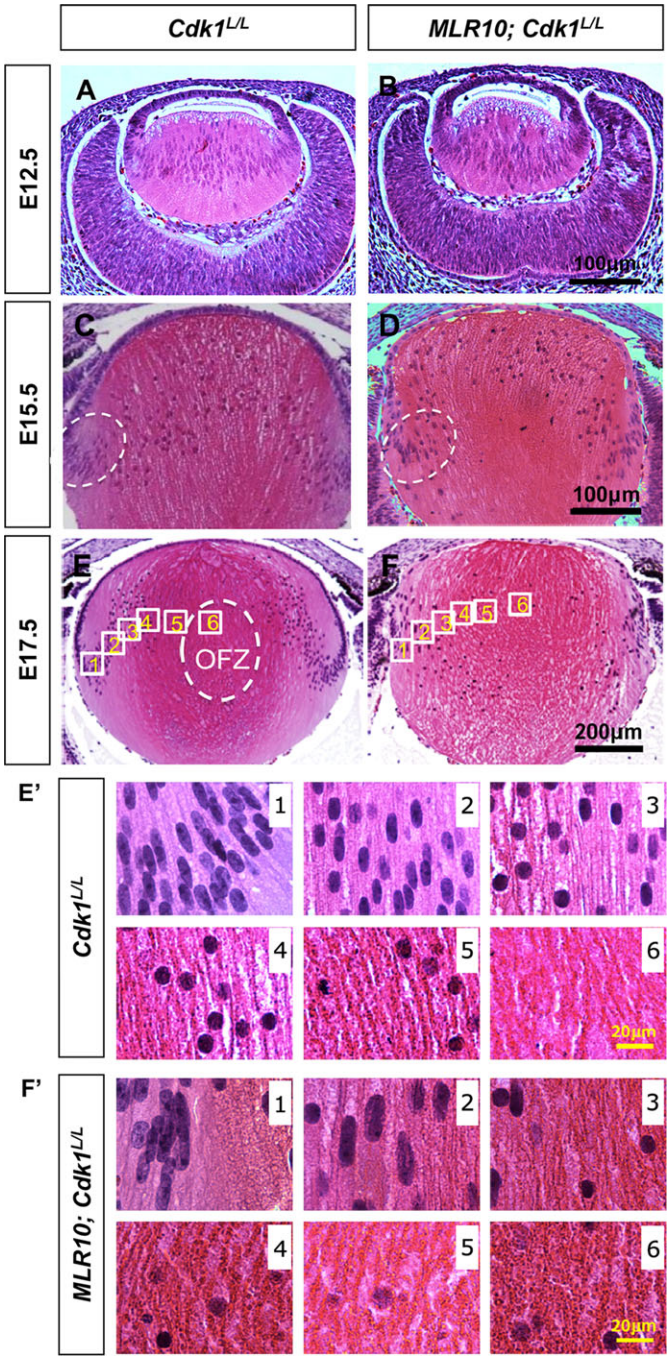

Fig. 3. The formation of an organelle-free zone requires CDK1. (A-F′) Hematoxylin and Eosin staining of the lenses at E12.5 (A,B), E15.5 (C,D) and E17.5 (E,F) with boxed zones designated 1-6 indicating comparable areas within the fiber cell mass shown at 10-fold higher magnification (E′,F′). At E12.5, Cdk1$^{L/L}$ control (A) and *MLR10; Cdk1$^{L/L}$* (B) lenses appeared morphologically indistinguishable. At E15.5, the *MLR10; Cdk1$^{L/L}$* lens fibers in the bow region contained larger nuclei than comparable fiber cells in the control bow region (compare nuclei in the dashed ovals of D,C). The cortical secondary fiber cell nuclei of *MLR10; Cdk1$^{L/L}$* lenses were fewer in number and larger than those of the control lens at E17.5 (F′ and E′, compare zones 1 and 2). Although the nuclear size of *MLR10; Cdk1$^{L/L}$* fiber cells normalized, the nuclear density remained lower than the control lens in zones 3-5 (F′,E′). By E17.5, an organelle-free zone (OFZ), devoid of nuclei, had formed in the control lenses (dashed oval in E and zone 6 in E′) but nuclei persisted in the *MLR10; Cdk1$^{L/L}$* lenses (zone 6, F′). Scale bars: 100 μm in A-D; 200 μm in E,F and 20 μm in E′,F′.

at the bow region of *MLR10; Cdk1$^{L/L}$* lenses appeared 152% larger by cross-sectional area, relative to those of control littermates (Fig. 3, compare the size of nuclei in the dashed ovals in D with those in C).

Mouse fiber cells normally begin losing their nuclei at approximately E16-18 (Kuwabara and Imaizumi, 1974). Consistent with this observation, lenses with intact *Cdk1* excluded nuclei from central fibers from E17.5 onwards (Fig. 3E, dashed oval, E′, zone 6). By contrast, E17.5 *MLR10; Cdk1$^{L/L}$* lenses retained nuclei in the center of the lens, resulting in a failure to form an OFZ (Fig. 3F,F′, see persistent nuclei in zone 6). Bassnett and others documented descriptive criteria for nuclei during the lens fiber cell differentiation

Development (2014) 141, 3388-3398 doi:10.1242/dev.106005

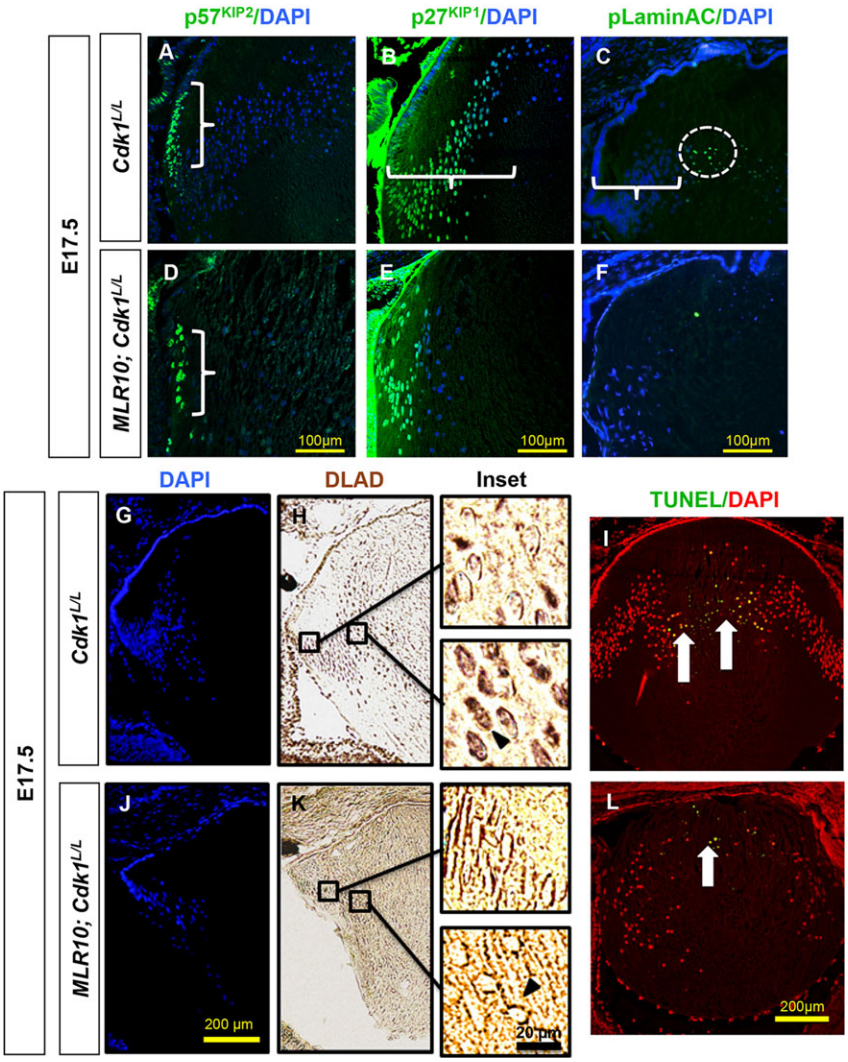

Fig. 4. CDK1 deficiency decreased the phosphorylation of lamin A/C, blocked the entry of DLAD into the nucleus and decreased DNA degradation in maturing lens fiber cells. (A-H,J,K) Primary antibodies to $p57^{KIP2}$ (A,D), $p27^{KIP1}$ (B,E), pLamin A/C (C,F) and DLAD (H,K) were used on E17.5 $Cdk1^{L/L}$ (A,B,C,G,H) and *MLR10; Cdk1*$^{L/L}$ (D,E,F,J,K) lens sections to detect appropriate antigens. (I,L) TUNEL analysis on E17.5 $Cdk1^{L/L}$ (I) and *MLR10; Cdk1*$^{L/L}$ (L) lens sections revealed DNA degradation. (A,D) $p57^{KIP2}$ expression (green stained nuclei) initiated in transitional zone epithelial cells in both control ($Cdk1^{L/L}$) and *Cdk1*-deficient (*MLR10; Cdk1*$^{L/L}$) lenses but declined quickly as fiber cells elongated (bracket). (B,E) By contrast, $p27^{KIP1}$ persisted in the nuclei of fiber cells deep into the cortex of the control lens (bracket in B) but remained more cortical in the *MLR10; Cdk1*$^{L/L}$ lenses (E). (C) Lamin A/C phosphorylation (green foci, dashed circle) initiated near the center of the lens where the organelle-free zone is forming. (H,I) In the same region where pLamin A/C is detected in the control lenses, both DLAD-positive nuclei (lower right inset, H) and TUNEL-positive foci (I, yellow staining, arrows) are found. (F,K,L) *MLR10; Cdk1*$^{L/L}$ lenses do not contain pLamin A/C (F), display reduced TUNEL-positive fiber cell foci (L, yellow staining, arrow) and exhibit DLAD accumulation around rather than within late fiber cell nuclei (lower right inset, K). Upper right insets in H and K are high magnifications of cortical fiber cells where DLAD expression is comparatively weak; lower right insets are high magnifications of more mature fiber cells where DLAD expression is clearly evident. Nuclei are counterstained with DAPI, which is blue in A-G,J but pseudocolored red in I and L to enhance the contrast for the TUNEL assay. Scale bars: 100 μm in A-F; 200 μm in G-L; 20 μm in H,K (insets).

process. We used these criteria to distinguish the nuclei in E17.5 *MLR10; Cdk1*$^{L/L}$ and control lenses (Bassnett, 2009). The youngest secondary fiber cells, near the lens equator in zone 1, possessed densely packed elongated oval nuclei in control lenses (Fig. 3E,E′, zone 1). In zone 1 of the *MLR10; Cdk1*$^{L/L}$ lens, the fiber cell nuclei were also oval, but fewer in number and their average cross-sectional area was 172% larger than those of control lenses (Fig. 3, compare zone 1 in F′ with E′). From E17.5 onwards, distinctly fewer cells appeared to undergo secondary fiber cell differentiation in the *MLR10; Cdk1*$^{L/L}$ lenses.

In zone 2, the nuclei in the fibers of control lenses were more sparse and less elongated than in zone 1 (Fig. 3E, compares zone 1 and 2). CDK1-deficient lenses also contained relatively fewer nuclei in zone 2 but they appeared considerably larger than the comparable region in the control lens (Fig. 3F′,E′, compare zones 2) and virtually unchanged in size from zone 1 (Fig. 3F′, compare zones 1 and 2). In zone 3, the control fiber nuclei assumed a smaller, more-rounded shape (compared to zones 1 and 2) and also stained more darkly with Hematoxylin (suggestive of nuclear condensation). The CDK1-deficient fibers of zone 3 contained a mixture of large, elongated, more-rounded nuclei that appeared similar, in size and shape, to the zone 3 nuclei of control fiber cells (Fig. 3E′,F′, compare zones 3). Sparsely packed spherical nuclei, similar in size to those in zone 3, persisted in the control lenses in zones 4 and 5 (Fig. 3E′, zones 4, 5). The *MLR10; Cdk1*$^{L/L}$ fiber nuclei appeared fewer in number with more variable size in zones 4 and 5 (compared with the control) and this pattern persisted into zone 6 (Fig. 3F′). By contrast, zone 6 of the control lens was devoid of nuclei (Fig. 3E′, zone 6).

Loss of CDK1 prevents entry of DLAD into the nucleus of terminally differentiating lens fiber cells

The entry of DLAD into the nuclear compartment requires the disassembly of the nuclear membrane, which normally occurs as fiber cells approach the OFZ. Analogous to mitotic events, we postulated that the nuclear membrane might remain intact in fiber cells lacking CDK1, thus preventing the entry of DLAD. CDK activity is controlled by cyclin-dependent kinase inhibitors. As lens epithelial cells begin to differentiate, they express $p27^{KIP1}$ and $p57^{KIP2}$, and both of these CDK inhibitors cooperate in the initiation of cell cycle withdrawal during embryonic fiber cell differentiation (Zhang et al., 1998; Lovicu and McAvoy, 1999; Nagahama et al., 2001; Kase et al., 2005). In keeping with these reports, both control and *MLR10; Cdk1*$^{L/L}$ lens epithelial cells express $p57^{KIP2}$ prior to reaching the lens equator; however, expression in both genotypes abruptly ends as the cells begin to detach from the lens capsule (Fig. 4, compare bracketed region in A and D). By comparison, the expression of $p27^{KIP1}$ extends further into the fiber cell mass than $p57^{KIP2}$ in control lenses (Fig. 4B, bracketed region), and becomes undetectable just prior to nuclear degradation in the OFZ. Additional

Development (2014) 141, 3388-3398 doi:10.1242/dev.106005

coordinated events that occur prior to the formation of the OFZ in control lenses include the nuclear concentration of CDK1 (Fig. 1, zones 3, 4), the adoption of a spherical nuclear morphology (Fig. 3E′, zones 4, 5), the disappearance of $p27^{KIP1}$ (Fig. 4B), and the phosphorylation of nuclear lamins A and C (Fig. 4C). In CDK1-deficient lenses, $p57^{KIP2}$ and $p27^{KIP1}$ are also observed in the outer regions, but $p27^{KIP1}$ expression is below detection limits in the inner fiber cell mass (Fig. 4, compare E with B). In addition, CDK1-deficient nuclei fail to exhibit phosphorylation of Lamin A/C (Fig. 4, compare F with C).

Concurrent with the onset of phosphorylation of lamin A/C in control lenses, DLAD moves from the periphery of the nucleus to within the nucleus (Fig. 4H). As indicated in the top inset panel, there is little DLAD evident in early nucleated fiber cells. By contrast, as indicated in the bottom inset panel, uniform DLAD staining is observed throughout the nuclei just prior to the formation of the OFZ. The entrance of DLAD in control lenses anticipates the DNA degradation as shown by abundant TUNEL-positive foci in the developing OFZ (Fig. 4I, yellow staining, arrows). Although DLAD generates 3′-phosphoryl/5′-hydroxyl ends following endonucleic cleavage of DNA (Shiokawa and Tanuma, 1999), endogenous phosphatases rapidly convert the 3′-PO_4^- ends to 3′-OH ends that can be labeled by the TUNEL assay (De Maria and Bassnett, 2007). By contrast, in *MLR10; Cdk1*$^{L/L}$ lenses, DLAD accumulated around the periphery of central fiber cell nuclei, rather than entering the nucleus, as seen in the control lenses (Fig. 4, compare the lower inset of K with the lower inset of H), and fewer fiber cell nuclei demonstrate degradation of DNA (Fig. 4, compare yellow nuclei in L to I).

Relocalization of NuMA during fiber cell differentiation and maturation

The nuclear mitotic apparatus protein (NuMA) is mechanistically involved in chromosome segregation that precedes nuclear disassembly and mitosis (Gribbon et al., 2002; Abad et al., 2007; Kotak and Gonczy, 2014). During the metaphase-anaphase transition, CDK1-induced phosphorylation on threonine 2055 (T2055) results in movement of NuMA from the cell membrane to the spindle poles, resulting in chromosome segregation (Kotak et al., 2013). Western analysis indicated the presence of pNuMA in control lenses (Fig. 5C). Immunohistochemical analyses confirmed the presence of pNuMA in control, *Cdk1*$^{L/L}$, lenses (Fig. 5A1-3). In these lenses, pNuMA is observed distributed or as multiple foci throughout the entire nuclei of epithelial cells and early differentiating fiber cells (Fig. 5A1). Consistent with a role for pNuMA in organizing chromatin, fewer prominent pNuMA puncta are observed in more differentiated fibers (Fig. 5A2) of the control lens and this is echoed by the punctate pattern of chromatin staining (Fig. 3E1-3 and Fig. 5A1-3; supplementary material Fig. S2B, specifically #2-4). Strikingly, however, rather than coalescing to a few or to two prominent foci as they do in mitosis, in *Cdk1*$^{L/L}$ control mouse lenses they appear to coalesce to a single large focus in the denucleating cells (Fig. 5A3). By comparison, pNuMA was present at considerably lower levels in western blots in *MLR10; Cdk1*$^{L/L}$ lenses and it was below the limit of immunofluorescent detection in the CDK1-deficient lens fiber cells (Fig. 5B1-3). Some pNuMA was observed in a few epithelial cells in these lenses (Fig. 5B). Consistent with an absence of pNuMA foci in the *MLR10; Cdk1*$^{L/L}$ lens, the nuclei remain larger and the chromatin

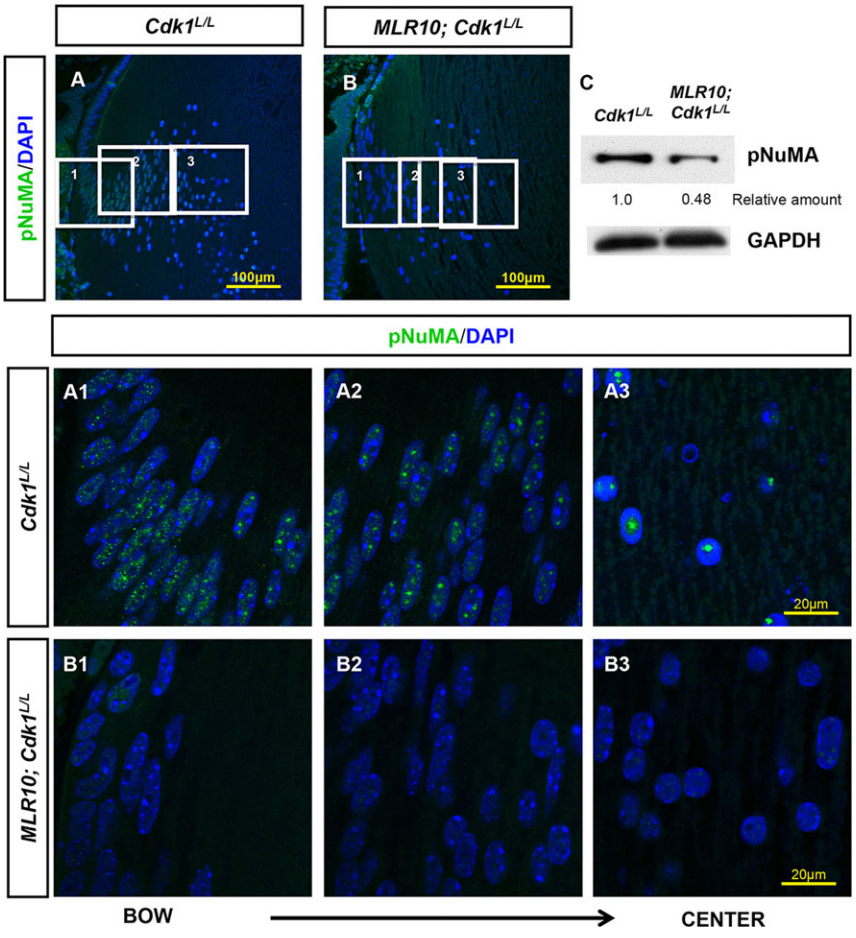

Fig. 5. Lenses deficient in CDK1 failed to phosphorylate NuMA. (A-C) The monoclonal anti-phosphorylated threonine 2055 of NuMA (pNuMA) antibody detected the presence of pNuMA in *Cdk1*$^{L/L}$ lenses (A,C), and *MLR10; Cdk1*$^{L/L}$ lenses at E16.5 (B,C). Immunofluorescent (A,B) and western blot analysis (C) revealed reduced pNuMA in *MLR10; Cdk1*$^{L/L}$ lenses (B,C) relative to *Cdk1*$^{L/L}$ lenses (A,C). Three regions of *Cdk1*$^{L/L}$ (A, white boxes 1-3) and *MLR10; Cdk1*$^{L/L}$ (B, white boxes 1-3) lenses were selected for magnification (A1-3, B1-3, respectively). At the bow region of *Cdk1*$^{L/L}$ lenses, pNuMA diffusely spread across the entire nucleus (A1). As fiber cells mature towards the center of *Cdk1*$^{L/L}$ lenses, pNuMA localization appeared more punctate, finally converging on a single focus in the most mature fiber cell nuclei (A2,A3). By contrast, *MLR10; Cdk1*$^{L/L}$ lenses exhibit low levels of pNuMA post-mitotically, as both peripheral (B1) and central fibers (B3) lack pNuMA staining. Scale bars: 100 μm in A,B; 20 μm in A1-3,B1-3.

Development (2014) 141, 3388-3398 doi:10.1242/dev.106005

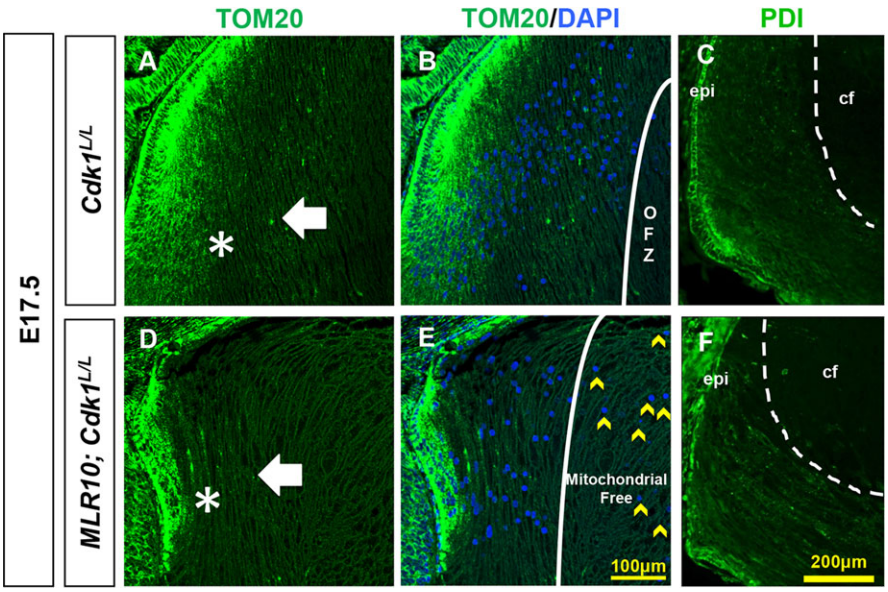

Fig. 6. *MLR10; Cdk1$^{L/L}$* lenses remove both mitochondria and endoplasmic reticulum, despite retaining nuclei. Mitochondria were detected by Tom20 (A,B,D,E) and endoplasmic reticulum by PDI (C,F) immunofluorescence (green staining) in E17.5 lenses. *Cdk1$^{L/L}$* (A-C) and *MLR10; Cdk1$^{L/L}$* (D-F) lens fiber cells lose their mitochondria (A,B,D,E) and endoplasmic reticulum (C,F) prior to reaching the center of the lens. Tom20 staining drops precipitously outside the most peripheral fiber cells (asterisks in A,D) but remains as punctate foci until the deep fiber cells of the central zone (arrows in A,D). *Cdk1$^{L/L}$* lenses form an organelle-free zone (OFZ) lacking both mitochondria and nuclei (B). The *MLR10; Cdk1$^{L/L}$* central lens fibers lack mitochondria, but retain nuclei (E, yellow arrowheads). Likewise, both control (C) and *MLR10; Cdk1$^{L/L}$* (F) lenses remove PDI-staining endoplasmic reticulum from mature nuclear fiber cells (lack of green staining within the dotted line border in C,F). Nuclei were counterstained with DAPI (B,E). Scale bars: 100 μm A,B,D,E; 200 μm C,F. epi, lens epithelium; cf, central fiber cells.

remains heterogeneously spread or less focused throughout the nucleus (Fig. 3F1 and Fig. 5B1-3; supplementary material Fig. S2C,D). Interestingly, total NuMA was also decreased in the CDK1-deficient lens (supplementary material Fig. S4).

Specificity of nuclear retention in CDK1 deficient lenses

Despite retaining fiber cell nuclei, CDK1-deficient lenses removed mitochondria from central fiber cells, as indicated by diminished Tom20 (an outer mitochondrial membrane protein) immunoreactivity in fiber cells (Fig. 6, asterisks in A,D). Some mitochondria remained in outer fibers but disappeared in the central fiber cells in both genotypes (Fig. 6, white arrows in A,D). Immunostaining for the endoplasmic reticulum marker protein disulfide isomerase, PDI, also appeared similar between the *MLR10;Cdk1$^{L/L}$* and the control mice (Fig. 6C,F), and no endoplasmic reticulum is indicated in mature central fiber cells (Fig. 6, inside dotted border C,F). This contrasts with the prolonged expression of PDI in lenses from dominant-negative *Ncoa6* transgenic mice that also exhibit retention of nuclei in lens fiber cells (Wang et al., 2010). Thus, although mitochondria (Fig. 6A,D) and endoplasmic reticulum (Fig. 6C,F) were destroyed in both genotypes, only *MLR10; Cdk1$^{L/L}$* lenses retained nuclei in central fiber cells (Fig. 6E, yellow arrowheads), consistent with the hypothesis that CDK1 deficiency specifically inhibits denucleation rather than causing a generalized inhibition of organelle destruction.

Epithelial cells in *Cdk1*-deficient lenses fail to undergo mitosis, and exhibit DNA endoreduplication

Although the number and density of lens epithelial cell nuclei were similar in the control and *MLR10; Cdk1$^{L/L}$* lenses at E12.5 (Fig. 7E), by E15.5 there were fewer total epithelial cell nuclei, and fewer epithelial cell nuclei per unit area, in *MLR10; Cdk1$^{L/L}$* lenses than in control lenses (Fig. 7, compare B with A,D and C,E). There was, however, no increase in epithelial cell apoptosis in CDK1-deficient lenses at E15.5 or E17.5 (Fig. 4I,L; supplementary material Fig. S3B-D). Therefore, decreased cell survival fails to explain the loss of epithelial cell population density in the *MLR10; Cdk1$^{L/L}$* lens.

As CDK1 plays an essential role in cell cycle regulation, assays for BrdU incorporation (an S-phase indicator) and phosphorylated histone H3 (pHH3) (a marker of late G2 phase, immediately prior to mitosis) were used to assess the cell cycle in *MLR10; Cdk1$^{L/L}$* lenses. *MLR10; Cdk1$^{L/L}$* lenses exhibited an S-phase index (proportion of BrdU positive nuclei) similar to that of control lenses at both E12.5 and E15.5 (Fig. 8, compare B with A, solid bars in I). However, by E17.5, epithelial cells in the *MLR10; Cdk1$^{L/L}$* lens displayed a significantly higher S-phase index, despite the decreased cell density of the epithelial cell layer. Likewise, starting at E15.5 and continuing to at least E17.5, a significantly higher percentage of lens epithelial cells in *MLR10; Cdk1$^{L/L}$* mice exhibit pHH3 immunoreactivity than in age-matched control mice (Fig. 8, compare F with E, H with G, lightly shaded bars in I). As *MLR10; Cdk1$^{L/L}$* lens epithelial cells exhibited both BrdU incorporation and pHH3 expression, the cell cycle appeared to be active in these epithelial cells. However, the widespread expression of pHH3 in *MLR10; Cdk1$^{L/L}$* lens epithelial cells suggested that although the mutant lens nuclei prepare to leave G2, they may not actually enter mitosis. Consistent with this hypothesis, we observe a 265% increase in nuclear cross-sectional area in comparison with control lens epithelial cell nuclei (Fig. 8, compare K with J,L). The reduced number of lens epithelial cells coupled with the increased nuclear size suggests that CDK1-deficient lens epithelial cells bypass mitosis and simply undergo endoreduplication of their DNA during the cell cycle. This also explains the reduced number of, and larger, nuclei in the differentiating secondary fiber cells of *MLR10; Cdk1$^{L/L}$* lenses.

DISCUSSION

In mammals, destruction or extrusion of nuclei occurs as a normal event during differentiation only in erythrocytes, keratinocytes and lens fiber cells. Of these, only lens fiber cells destroy nuclei within the cell. Despite many investigations over the past century, the molecular mechanism(s) by which fiber cell denucleation occurs has remained a mystery (Vrensen et al., 1991, 2004; He et al., 1998, 2010; Ivanov et al., 2005; Xie et al., 2007; Rivera et al., 2009; Wang et al., 2010; Gupta et al., 2011; Ma et al., 2011; Jarrin et al., 2012; Rodrigues et al., 2013). Preliminary work suggested that the lens 'appropriates' normal mitotic mechanisms in order to accomplish denucleation: specifically, that nuclear membrane disassembly occurs after phosphorylation of nuclear lamins and that stabilization of the CDK1 inhibitor p27^{KIP1} delays denucleation (Caceres et al., 2010). Furthermore, the persistence of CDK1 and its activator cyclin B and entry of DLAD, while p27^{KIP1} levels decline (He et al., 1998) (Figs 1 and 4), as well as observations of delayed

Development (2014) 141, 3388-3398 doi:10.1242/dev.106005

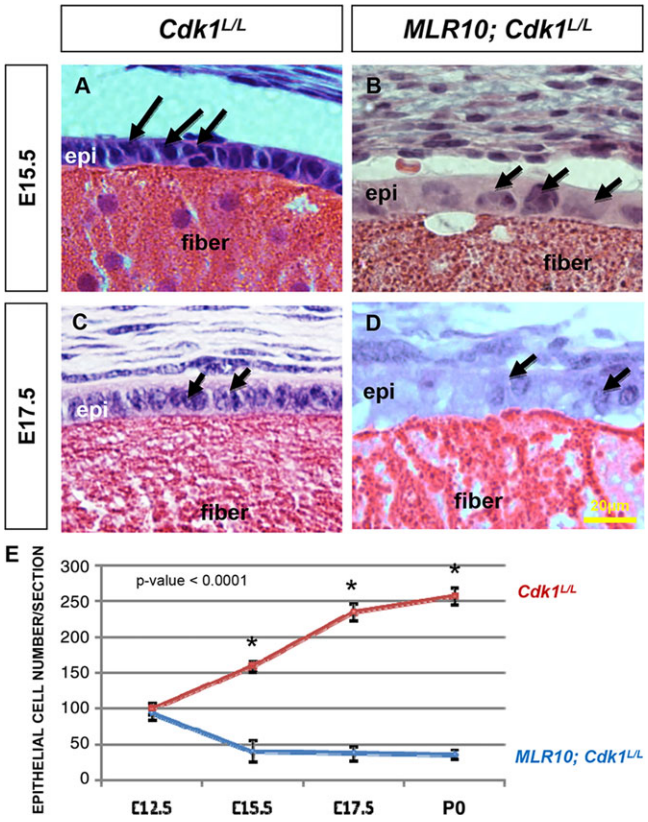

Fig. 7. CDK1-deficient lenses exhibited large, sparse epithelial cell nuclei. *Cdk1*$^{L/L}$ (A,C) and *MLR10; Cdk1*$^{L/L}$ (B,D) lenses at E15.5 (A,B) or E17.5 (C,D) were stained with Hematoxylin and Eosin. (A,B) At E15.5, the *MLR10; Cdk1*$^{L/L}$ lens epithelium contained fewer nuclei that appeared larger (B) than those in the *Cdk1*$^{L/L}$ control epithelium (A). (C,D) This relative epithelial cell reduction continued in *MLR10; Cdk1*$^{L/L}$ lenses at E17.5 (compare D with C). (E) Since the *MLR10; Cdk1*$^{L/L}$ and *Cdk1*$^{L/L}$ lenses were similar in size, the number of lens epithelial cell nuclei per section was used as an indicator of lens epithelial cell population size. At embryonic day 12.5 (E12.5) lens epithelial sections contained comparable numbers of nuclei in both control and CDK1-deficient lenses, but by E15.5 the number of lens epithelial cell nuclei present in the *MLR10; Cdk1*$^{L/L}$ lenses actually declined, whereas the epithelial cell number increased in the control lenses. The lens epithelial nuclei per section continued to diverge between *MLR10; Cdk1*$^{L/L}$ and control lens through P0. Each data point represents the mean ± s.e.m. with nine measurements (three sections from each of three different embryos). Scale bars: 20 µm. epi, lens epithelium; fiber, lens fiber cells. Arrows highlight selected epithelial nuclei to emphasize the difference in nuclear size and population density between the *MLR10; Cdk1*$^{L/L}$ and control lens epithelium.

denucleation in DLAD$^{-/-}$ mice (Nishimoto et al., 2003), all suggested that CDK1 directs fiber cell denucleation. In proof of principle experiments, here we show that the phosphorylation of lamin, entry of DLAD in to the nuclear compartment and denucleation per se require CDK1, thus elucidating upstream events leading towards lens fiber denucleation. Focalization of pNuMA appears to be a consequence of CDK1 activity.

As germline deletion of *Cdk1* results in pre-implantation lethality (Santamaria et al., 2007), the *MLR10* CRE transgene was exploited to remove *Cdk1* specifically from the lens (Fig. 2). Whereas normal fiber cells exhibited phosphorylation of the known CDK1 substrate lamin A/C in the region just prior to fiber cell denucleation, it remained unphosphorylated in CDK1-deficient fiber cells. Furthermore, in the absence of CDK1, DLAD remained outside the fiber cell nuclei (Fig. 4K, lower inset) and these cells failed to denucleate (Fig. 3D,F,F′). Taken together, these findings indicate that fiber denucleation requires CDK1 activity. The specificity of the requirement of CDK1 for removal of nuclei per se is implied by observations that breakdown of the mitochondria and endoplasmic reticulum occurred on schedule in *MLR10; Cdk1*$^{L/L}$ lens fibers (Fig. 6).

NuMA is a CDK1-dependent regulator of mitosis. Although elucidation of regulation of its function remains in progress, it is clear that, during mitosis, CDK1-dependent phosphorylation causes NuMA to concentrate at spindle poles and to induce a redistribution of dynein that results in chromosome segregation and eventually the division of the nucleus (Lelievre et al., 1998; Abad et al., 2007; Kotak et al., 2013; Zheng et al., 2014). Data in Fig. 5 indicate that NuMA is also involved in the chromatin organization that precedes lens fiber denucleation (Fig. 5A1-3; supplementary material Fig. S2). Interestingly, whereas in mitotic cells two foci are formed, in denucleating lens cells only a single large pNuMA focus is observed in these wild-type mice. By contrast, NuMA T2055 remained largely unphophorylated in CDK1-deficient fiber cells, and chromatin was less consistently organized (Fig. 5B1-3; supplementary material Fig. S2). Together, the data suggest that lens fiber cells appropriate from normal mitosis the crucial function of CDK1-driven phosphorylation of lamin and NuMA in order to direct lens cell denucleation and development. Whereas in mitosis CDK1 drives the coordinated disassembly of the nuclear membrane and organization of chromatin to allow for formation of daughter cells, in lens fibers chromatin and nuclei are destroyed. In addition to directing phosphorylation and localization of NuMA, CDK1 seems to regulate the levels of the native protein and this may be related to the levels of the pNuMA. The relationship between CDK1 and NuMA is consistent with a feedback mechanism. Elucidation of additional steps in regulation of these events during lens development will be the topic of future investigations.

Interestingly, *MLR10; Cdk1*$^{L/L}$ lenses contained fewer nuclei in both the epithelium (Fig. 7) and fiber cells (Figs 3 and 4) than controls, despite exhibiting retention of fiber cell nuclei in the putative OFZ. The reduction in total fiber cells and nuclei in the *MLR10; Cdk1*$^{L/L}$ lens appears to result from a reduction in epithelial cells required to fuel continued secondary fiber cell differentiation (Figs 2 and 3). Furthermore, the loss of lens epithelial cells in CDK1-deficient lenses occurred without detectable increases in apoptosis, suggesting that CDK1 is dispensable for lens cell survival (Fig. 4; supplementary material Fig. S3). In addition, in *MLR10; Cdk1*$^{L/L}$ lenses, there was no extensive migration of the lens posterior epithelium, as observed in lens fibers in which DNA damage repair is compromised (Wang et al., 2010). If it is assumed that apoptosis is a consequence of DNA damage, these data suggest CDK1-driven entry of DLAD into the nucleus, and the initial disassembly of DNA, operate upstream of the requirements for retention of DNA integrity.

Another remarkable feature of *MLR10; Cdk1*$^{L/L}$ lenses is the disparate size of primary versus secondary fiber cell nuclei (Fig. 3D,F versus 3C,E). Nuclei within inner fiber cells of both genotypes (including nuclei of what should be the OFZ in *MLR10; Cdk1*$^{L/L}$) are of similar dimensions. (Fig. 3, compare zones 4-6 in F′ with zones 4 and 5 in E′). However, nuclei in outer fibers of CDK1-deficient lenses, though fewer in number, appear distinctly larger (Fig. 3, compare zones 1 and 2 in F′ with zones 1 and 2 in E′; Fig. 4, compare the p57^{KIP2}-positive nuclei in D with those in A). We posit that this difference in the size of primary versus secondary fiber cell nuclei in *MLR10; Cdk1*$^{L/L}$ lenses results from a difference in the number of genomic duplications experienced by the two different populations

Development (2014) 141, 3388-3398 doi:10.1242/dev.106005

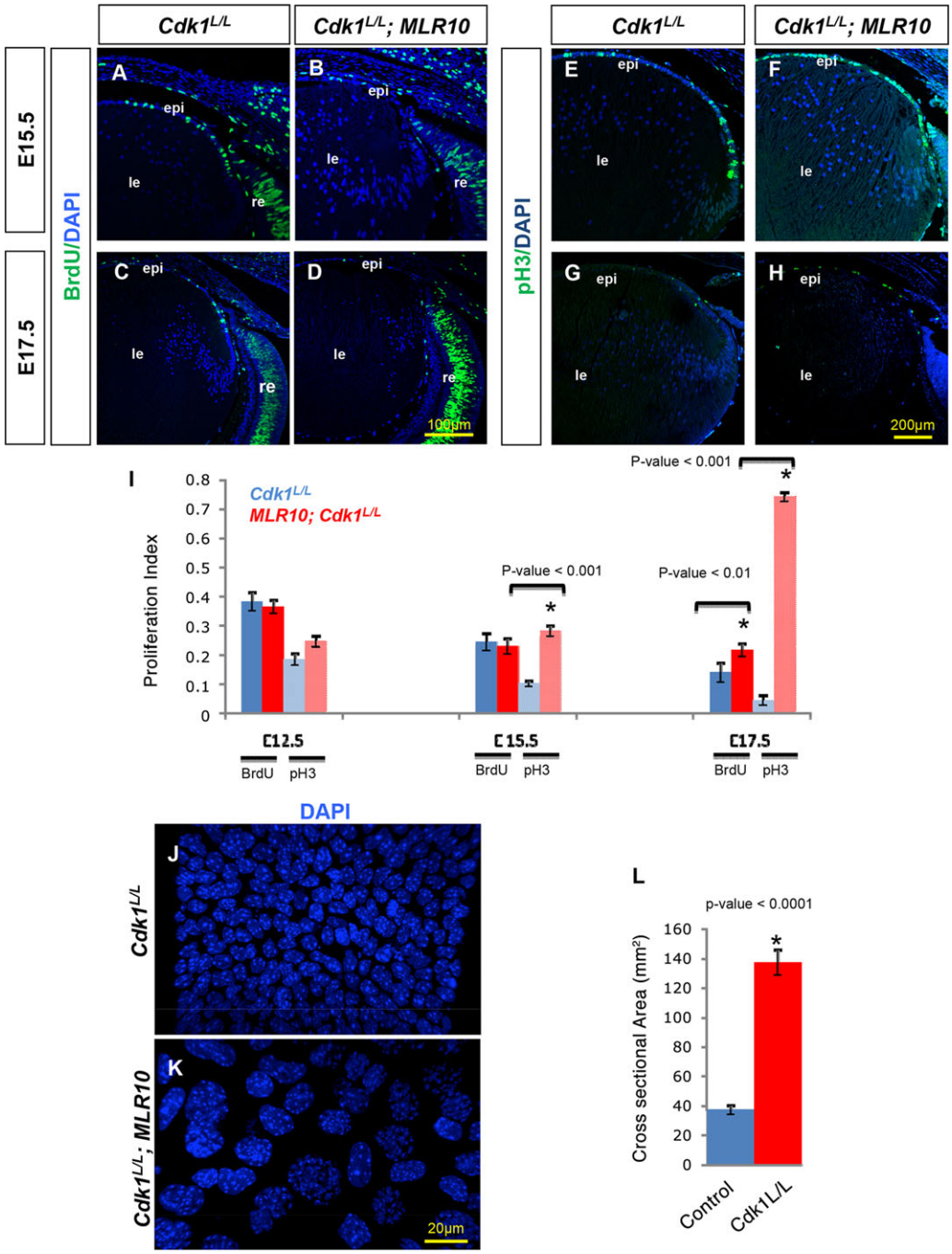

Fig. 8. *MLR10; Cdk1*$^{L/L}$ lens epithelial cells continue to synthesize DNA but fail to enter mitosis. (A-H) BrdU incorporation and phosphorylated histone H3 (pHH3) immunohistochemistry (green nuclei) were used to determine the proportion of cells in S phase (A-D) and late G2 phase (E-H), respectively. Nuclei were counterstained with DAPI. The proliferation index (S-phase fraction) did not differ significantly between *MLR10; Cdk1*$^{L/L}$ and *Cdk1*$^{L/L}$ lenses at E12.5 or at E15.5 (compare B with A, solid bars in I) but significantly increased in *MLR10; Cdk1*$^{L/L}$ lenses by E17.5 (compare D with C, solid bars in I). Although there were fewer overall BrdU-positive nuclei in the *MLR10; Cdk1*$^{L/L}$ lenses, the proportion of total nuclei that were BrdU positive was relatively increased at E17.5. The proportion of pHH3-positive cells levels were significantly higher in *Cdk1*-deficient lenses beginning at E15.5 (compare E with F, lightly shaded bars in I) and most remaining epithelial cells in *MLR10; Cdk1*$^{L/L}$ lenses stained positive for pHH3 by E17.5 (compare H with G, lightly shaded bars in I). (J,K) Whole lenses from *Cdk1*$^{L/L}$ (J) and *MLR10; Cdk1*$^{L/L}$ mice (K) were stained with DAPI, and the intact epithelium was visualized by confocal microscopy to visualize the size and density of epithelial nuclei. (K,L) *MLR10; Cdk1*$^{L/L}$ lenses exhibited a significant increase in nuclear size and an increased DAPI staining foci in each cell. All bars represent the mean ± s.e.m., with each bar representing nine measurements (three sections from each of three different embryos). Scale bars: 100 μm in A-D; 200 μm in E-H; 20 μm J,K. le, lens; re, retina; epi, lens epithelium.

of precursor cells, as well as poorer organization due to limited NuMA, as noted above. As the deletion of the floxed *Cdk1* allele commences at E10.5, the older, primary fiber cells would largely have been in the process of withdrawing from the cell cycle before the knock down of CDK1 was taking effect. By contrast, the future secondary fiber cells would still be epithelial cells at E10.5 and would likely go through one or more rounds of DNA synthesis before withdrawing from the cell cycle. The large secondary fiber cell nuclei

Development (2014) 141, 3388-3398 doi:10.1242/dev.106005

in *MLR10; Cdk1*$^{L/L}$ lenses precisely match the phenotype expected if lens epithelial cells underwent endoreduplication of DNA without mitosis in the absence of CDK1 prior to differentiation. This is supported by the higher proliferation index of CDK1-deficient lens epithelial cells (Fig. 8). Furthermore, the higher proportion of *MLR10; Cdk1*$^{L/L}$ lens epithelial cells in S-phase or G2 phase and that are enlarged (Figs 7 and 8) is consistent with previous studies documenting the requirement of CDK1 for nuclear disassembly in mitosis and meiosis during development (Adhikari et al., 2012). Likewise, *Cdk1* null pre-implantation mouse embryos that reach the blastocyst stage and mouse embryonic fibroblasts conditionally deleted for *Cdk1* exhibit a reduced number of (abnormally large) nuclei (Santamaria et al., 2007; Diril et al., 2012).

In conclusion, this discovery of a requirement for CDK1 activity for a terminal differentiation pathway, including removal of nuclei and establishing an OFZ, expands the known functions for this protein beyond those for mitosis and meiosis. In the lens, CDK1 deficiency fails to induce apoptosis or prevent the onset of secondary fiber cell differentiation. The fundamental process of nuclear disassembly apparently requires lamin phosphorylation by CDK1 and includes NuMA-related chromatin organization. The finding that these processes can occur independently of cell division implies that CDK1 may play important roles in other aspects of nuclear function. There are several disease-related laminopathies, including Emery-Dreifuss muscular dystrophy (EDMD), dilated cardiomyopathy (DCM), limb-girdle muscular dystrophy and Hutchinson-Gilford progeria syndrome, most of which profoundly affect non-proliferating cells (reviewed by Ho and Lammerding, 2012). This work suggests that CDK1, and perhaps other regulators of nuclear structure during mitosis, may play an unappreciated role in terminally differentiated cells.

MATERIALS AND METHODS

Mice

Mice were used in accordance with the ARVO statement for the Use of Animals in Ophthalmic and Visual Research. Transgenic mice expressing CRE in the lens fiber cells (*MLR39*) and in the entire lens (*MLR10*) have been described previously (Zhao et al., 2004). The *Cdk1*$^{L/L}$ mice were generated using a conditional targeting vector assembled on a pBluescript II KS(+) backbone (Stratagene). The targeted region of *Cdk1* contained exon 3 originally amplified with *Cdk1* primers containing engineered restriction sites (underlined) (forward, CGG GGT ACC TAG ATA GCT AGG GAA TCC GCA CCT GA; reverse, GCG TCC GGA GGC AGC TAC CAG AGG TGC TAA GTA AG) with flanking LoxP sites. The *Cdk1* 5′ arm contained exon 2, whereas the 3′ arm contained exons 4 and 5. The neomycin gene flanked by FRT sites was inserted into intron 2 as a selectable marker. Transfection of linearized pBluescript, screening of targeted TC-1 embryonic stem (ES) cells and injection of blastocysts to produce chimeric males were performed as described previously (Dix et al., 1996). Agouti male chimera offspring were mated with *C57BL/6NCrl* females and then backcrossed onto the *129S* genetic background. Experimental mice were maintained on a mixed genetic background segregating for alleles originating in *FVB/N*, *129S* and *C57BL/6NCrl* strains.

Histology and immunohistochemistry

The gestational age of experimental embryos was determined by vaginal plug detection, set at embryonic day 0.5 (E0.5). One hour prior to embryo collection, pregnant dams were administered (0.1 mg/g body weight) 5-bromo-2′-deoxyuridine (BrdU) dissolved in phosphate-buffered saline (PBS) at a concentration of 100 mg/ml. For paraffin wax-embedded sections, embryos were collected and fixed in 10% neutral buffered formalin (NBF). Standard protocols were used to process and embed tissues in paraffin wax before sectioning at 5 µm. For frozen sections, lenses were fixed in 4% neutral buffered paraformaldehyde for 90 min at 4°C, embedded in OCT, frozen and sectioned at 10 µm. Cryosections were permeablized in 0.05% Triton X-100/PBS for 2 min, blocked in 5% donkey serum and 5% BSA in PBS for 30 min at room temperature before being incubated with DLAD, phosphorylated lamin A/C or PDI antibodies. The primary antibody for DLAD was generated as previously described (Nakahara et al., 2007) and used at a dilution of 1:500 overnight at 4°C. The secondary antibody used for visualization of DLAD was conjugated goat anti-hamster (Jackson ImmunoResearch, 127-035-160; 1:250). Detection of DLAD was via DAB peroxidase substrate kit (Vector Labs, SK4100). Images were collected using an Olympus light microscope BX51. Primary antibodies for phosphorylated NuMA (at threonine 2055) have been described previously (Kotak et al., 2013). Primary antibodies for phosphorylated lamin AC, BrdU, p57^{KIP2} and CDK1 (ab58528, ab6326, ab4058, and ab7953, respectively) were obtained from Abcam. The primary antibody for p27^{KIP1} (BD610241) was obtained from BD Biosciences. Primary antibodies for Tom20 (sc-11415) and total NuMA (sc-48773) were obtained from Santa Cruz Biotechnology, whereas antibodies for phosphorylated histone H3 (Ser10) and PDI were obtained from Millipore (16-189) and Sigma-Aldrich (P7122), respectively. All primary and secondary antibodies were used at a 1:100 dilution, with the exception of DLAD (noted above), total NuMA and phosphorylated histone H3, which were used at a 1:50 dilution. Primary antibodies were detected using secondary antibodies attached to fluorescent probes (Alexa Fluor 488 goat anti-rabbit IgG, Alexa Fluor 546 goat anti-rat IgG, FITC for donkey anti-rabbit IgG, 711-095-152 and Cy3 for donkey anti-mouse IgG). Sections were counterstained with DAPI (Vector Labs, H-1200). Photomicrographs were captured on a Zeiss 710 Laser Scanning Confocal System at the Center for Advanced Microscopy and Imaging at Miami University. Standard Hematoxylin and Eosin-stained sections were used to analyze the structure of the lens, and images were captured using a Nikon TI-80 microscope.

Immunofluorescence quantification

Quantifying indirect immunofluorescent labeling on tissue sections has been previously described (Garcia et al., 2011; Plageman et al., 2011; Madakashira et al., 2012). All immunofluorescent assays were photographed with identical exposure times. ImageJ software was used to measure the signal intensity of the pixels (RGB) and given areas. ImageJ software allowed for the selection of the plot to be measured. The BrdU and TUNEL index represented the ratio of the lens cell nuclei positive for the mentioned markers over the total DAPI stained nuclei in the ocular lens.

Whole-mount epithelial cell *z*-stacks

Lenses from *MLR10; Cdk1*$^{L/L}$ and *Cdk1*$^{L/L}$ mice at embryonic day 17.5 were immediately fixed in 10% NBF for 1 h. After fixation, the lenses were washed in PBS and stained with DAPI. The lenses were then placed in between two coverslips with a drop of PBS and a series of images were collected at varying depths using the Zeiss 710 Laser Scanning Confocal System, and finally reconstructed into a three-dimensional image. The cross-sectional area of each individual nucleus was determined using IMAGEPRO software at the Center for Advanced Microscopy and Imaging at Miami University.

Western blot

Cdk1$^{L/L}$, *MLR39; Cdk1*$^{L/L}$ and *MLR10; Cdk1*$^{L/L}$ lenses were taken at birth. The epithelial cell layer and fiber cell mass were physically separated in *Cdk1*$^{L/L}$ and *MLR39; Cdk1*$^{L/L}$ lenses, and homogenized in RIPA buffer [50 mM Tris-HCl (pH 8.0), 150 mM NaCl, 1% NP40, 0.5% sodium deoxycholate, 0.1% SDS] with phosphatase and protease inhibitors (Pierce, catalog number 78440). The protein concentration was determined by BCA assay (Pierce, catalog number 23227). Protein lysates were separated on a 10% SDS-polyacrylamide gels and transferred to PVDF membranes (Millipore, catalog number IPVH10100), blocked with 5% non-fat dry milk for 1 h at room temperature and incubated overnight at 4°C with antibodies to CDK1 (1:2000, Abcam, ab7953) or pNuMA (1:1000; Kotak et al., 2013). After incubation with HRP-conjugated secondary antibody (1:1000; Cell Signaling Technology, 7074) for 2 h, the proteins were analyzed on X-ray films following the addition of the chemiluminescent substrate Lumiglo (Cell Signaling Technology, 7003).

Acknowledgements
We thank Dr Pierre Gönczy for the gift of the pNUMA antibody; Devin G. Bruney for technical assistance; Molly M. Schleicher, Sheldon Rowan and Adam S. LeFever for critical review of the manuscript; and Ales Cvekl for guidance.

Competing interests
The authors declare no competing financial interests.

Author contributions
B.R.C. coordinated the breeding and genotyping of the mice, collected and processed biological material, performed histology, immunohistochemistry and photography, assembled most of the figures and wrote the first draft of the manuscript. M.-L.C. performed western blot analysis and immunohistochemistry. F.S. provided insights to the experimental design, data analysis and helped edit the manuscript. T.M.C. and E.M.E. created and provided the floxed Cdk1 mice prior to publication. B.D.W. modified the genotyping strategy used to maintain the Cdk1 floxed mice and assisted in animal husbandry, genotyping and maintenance of records. M.N. and S.N. made and provided the anti-DLAD antibody. M.L.R. directed the experimental procedures, critically analyzed all the data, coordinated research funding for the project, assisted in writing the first and subsequent drafts, and acted as co-corresponding author. A.T. and F.S. developed the initial hypothesis about the role of Cdk1 and fiber cell denucleation, assisted in experimental design, provided research funding, assisted in writing the first and subsequent drafts, and acted as co-corresponding authors.

Funding
This work was supported, in part, by grants from The National Eye Institute [EY012995 (M.L.R.), EY013250, EY021212 (A.T.)]; The USDA contract 1950-510000-060-01A (A.T.); Alcon (A.T.); Johnson and Johnson Focused Giving (A.T.); and by the Intramural Research Program of the National Institutes of Health (NIH), National Institute of Environmental Health Sciences (E.M.E.). A.T. is currently the Morris Belkin Weizmann Visiting Professor. Deposited in PMC for release after 12 months.

Supplementary material
Supplementary material available online at
http://dev.biologists.org/lookup/suppl/doi:10.1242/dev.106005/-/DC1

References

Abad, P. C., Lewis, J., Mian, I. S., Knowles, D. W., Sturgis, J., Badve, S., Xie, J. and Lelievre, S. A. (2007). NuMA influences higher order chromatin organization in human mammary epithelium. *Mol. Biol. Cell* **18**, 348-361.

Adhikari, D., Zheng, W., Shen, Y., Gorre, N., Ning, Y., Halet, G., Kaldis, P. and Liu, K. (2012). Cdk1, but not Cdk2, is the sole Cdk that is essential and sufficient to drive resumption of meiosis in mouse oocytes. *Hum. Mol. Genet.* **21**, 2476-2484.

Bassnett, S. (2009). On the mechanism of organelle degradation in the vertebrate lens. *Exp. Eye Res.* **88**, 133-139.

Bassnett, S. and Mataic, D. (1997). Chromatin degradation in differentiating fiber cells of the eye lens. *J. Cell Biol.* **137**, 37-49.

Caceres, A., Shang, F., Wawrousek, E., Liu, Q., Avidan, O., Cvekl, A., Yang, Y., Haririnia, A., Storaska, A., Fushman, D. et al. (2010). Perturbing the ubiquitin pathway reveals how mitosis is hijacked to denucleate and regulate cell proliferation and differentiation in vivo. *PLoS ONE* **5**, e13331.

De Maria, A. and Bassnett, S. (2007). DNase IIbeta distribution and activity in the mouse lens. *Invest. Ophthalmol. Vis. Sci.* **48**, 5638-5646.

Diril, M. K., Ratnacaram, C. K., Padmakumar, V. C., Du, T., Wasser, M., Coppola, V., Tessarollo, L. and Kaldis, P. (2012). Cyclin-dependent kinase 1 (Cdk1) is essential for cell division and suppression of DNA re-replication but not for liver regeneration. *Proc. Natl. Acad. Sci. USA* **109**, 3826-3831.

Dix, D. J., Allen, J. W., Collins, B. W., Mori, C., Nakamura, N., Poorman-Allen, P., Goulding, E. H. and Eddy, E. M. (1996). Targeted gene disruption of Hsp70-2 results in failed meiosis, germ cell apoptosis, and male infertility. *Proc. Natl. Acad. Sci. USA* **93**, 3264-3268.

Garcia, C. M., Huang, J., Madakashira, B. P., Liu, Y., Rajagopal, R., Dattilo, L., Robinson, M. L. and Beebe, D. C. (2011). The function of FGF signaling in the lens placode. *Dev. Biol.* **351**, 176-185.

Gribbon, C., Dahm, R., Prescott, A. R. and Quinlan, R. A. (2002). Association of the nuclear matrix component NuMA with the Cajal body and nuclear speckle compartments during transitions in transcriptional activity in lens cell differentiation. *Eur. J. Cell Biol.* **81**, 557-566.

Gupta, R., Asomugha, C. O. and Srivastava, O. P. (2011). The common modification in alphaA-crystallin in the lens, N101D, is associated with increased opacity in a mouse model. *J. Biol. Chem.* **286**, 11579-11592.

He, H.-Y., Gao, C., Vrensen, G. and Zelenka, P. (1998). Transient activation of cyclin B/Cdc2 during terminal differentiation of lens fiber cells. *Dev. Dyn.* **211**, 26-34.

He, S., Pirity, M. K., Wang, W.-L., Wolf, L., Chauhan, B. K., Cveklova, K., Tamm, E. R., Ashery-Padan, R., Metzger, D., Nakai, A. et al. (2010). Chromatin remodeling enzyme Brg1 is required for mouse lens fiber cell terminal differentiation and its denucleation. *Epigenet. Chromatin* **3**, 21.

Ho, C. Y. and Lammerding, J. (2012). Lamins at a glance. *J. Cell Sci.* **125**, 2087-2093.

Imai, F., Yoshizawa, A., Fujimori-Tonou, N., Kawakami, K. and Masai, I. (2010). The ubiquitin proteasome system is required for cell proliferation of the lens epithelium and for differentiation of lens fiber cells in zebrafish. *Development* **137**, 3257-3268.

Ivanov, D., Dvoriantchikova, G., Pestova, A., Nathanson, L. and Shestopalov, V. I. (2005). Microarray analysis of fiber cell maturation in the lens. *FEBS Lett.* **579**, 1213-1219.

Jarrin, M., Mansergh, F. C., Boulton, M. E., Gunhaga, L. and Wride, M. A. (2012). Survivin expression is associated with lens epithelial cell proliferation and fiber cell differentiation. *Mol. Vis.* **18**, 2758-2769.

Kase, S., Yoshida, K., Ikeda, H., Harada, T., Harada, C., Imaki, J., Ohgami, K., Shiratori, K., Nakayama, K. I., Nakayama, K. et al. (2005). Disappearance of p27(KIP1) and increase in proliferation of the lens cells after extraction of most of the fiber cells of the lens. *Curr. Eye Res.* **30**, 437-442.

King, R. W., Jackson, P. K. and Kirschner, M. W. (1994). Mitosis in transition. *Cell* **79**, 563-571.

Kotak, S. and Gönczy, P. (2014). NuMA phosphorylation dictates dynein-dependent spindle positioning. *Cell Cycle* **13**, 177-178.

Kotak, S., Busso, C. and Gönczy, P. (2013). NuMA phosphorylation by CDK1 couples mitotic progression with cortical dynein function. *EMBO J.* **32**, 2517-2529.

Kuwabara, T. and Imaizumi, M. (1974). Denucleation process of the lens. *Invest. Ophthalmol.* **13**, 973-981.

Lelievre, S. A., Weaver, V. M., Nickerson, J. A., Larabell, C. A., Bhaumik, A., Petersen, O. W. and Bissell, M. J. (1998). Tissue phenotype depends on reciprocal interactions between the extracellular matrix and the structural organization of the nucleus. *Proc. Natl. Acad. Sci. USA* **95**, 14711-14716.

Lovicu, F. J. and McAvoy, J. W. (1999). Spatial and temporal expression of p57 (KIP2) during murine lens development. *Mech. Dev.* **86**, 165-169.

Ma, B., Sen, T., Asnaghi, L., Valapala, M., Yang, F., Hose, S., McLeod, D. S., Lu, Y., Eberhart, C., Zigler, J. S., Jr et al. (2011). betaA3/A1-Crystallin controls anoikis-mediated cell death in astrocytes by modulating PI3K/AKT/mTOR and ERK survival pathways through the PKD/Bit1-signaling axis. *Cell Death Dis.* **2**, e217.

Madakashira, B. P., Kobrinski, D. A., Hancher, A. D., Arneman, E. C., Wagner, B. D., Wang, F., Shin, H., Lovicu, F. J., Reneker, L. W. and Robinson, M. L. (2012). Frs2alpha enhances fibroblast growth factor-mediated survival and differentiation in lens development. *Development* **139**, 4601-4612.

Nagahama, H., Hatakeyama, S., Nakayama, K., Nagata, M., Tomita, K. and Nakayama, K. (2001). Spatial and temporal expression patterns of the cyclin-dependent kinase (CDK) inhibitors $p27^{Kip1}$ and $p57^{Kip2}$ during mouse development. *Anat. Embryol. (Berl.)* **203**, 77-87.

Nakahara, M., Nagasaka, A., Koike, M., Uchida, K., Kawane, K., Uchiyama, Y. and Nagata, S. (2007). Degradation of nuclear DNA by DNase II-like acid DNase in cortical fiber cells of mouse eye lens. *FEBS J.* **274**, 3055-3064.

Nigg, E. A. (1993). Targets of cyclin-dependent protein kinases. *Curr. Opin. Cell Biol.* **5**, 187-193.

Nishimoto, S., Kawane, K., Watanabe-Fukunaga, R., Fukuyama, H., Ohsawa, Y., Uchiyama, Y., Hashida, N., Ohguro, N., Tano, Y., Morimoto, T. et al. (2003). Nuclear cataract caused by a lack of DNA degradation in the mouse eye lens. *Nature* **424**, 1071-1074.

Orthwein, A., Fradet-Turcotte, A., Noordermeer, S. M., Canny, M. D., Brun, C. M., Strecker, J., Escribano-Diaz, C. and Durocher, D. (2014). Mitosis inhibits DNA double-strand break repair to guard against telomere fusions. *Science* **344**, 189-193.

Plageman, T. F., Jr, Zacharias, A. L., Gage, P. J. and Lang, R. A. (2011). Shroom3 and a Pitx2-N-cadherin pathway function cooperatively to generate asymmetric cell shape changes during gut morphogenesis. *Dev. Biol.* **357**, 227-234.

Rabl, C. (1899). Über den bau und die entwicklung der linse. III Teil: die lines der säugethiere. *Z. Wiss. Zool.* **67**, 1-138.

Reza, H. M., Nishi, H., Kataoka, K., Takahashi, Y. and Yasuda, K. (2007). L-Maf regulates p27kip1 expression during chick lens fiber differentiation. *Differentiation* **75**, 737-744.

Rivera, C., Yamben, I. F., Shatadal, S., Waldof, M., Robinson, M. L. and Griep, A. E. (2009). Cell-autonomous requirements for Dlg-1 for lens epithelial cell structure and fiber cell morphogenesis. *Dev. Dyn.* **238**, 2292-2308.

Rodrigues, P. M. G., Grigaravicius, P., Remus, M., Cavalheiro, G. R., Gomes, A. L., Martins, M. R., Frappart, L., Reuss, D., McKinnon, P. J., von Deimling, A. et al. (2013). Nbn and atm cooperate in a tissue and developmental stage-specific manner to prevent double strand breaks and apoptosis in developing brain and eye. *PLoS ONE* **8**, e69209.

Santamaría, D., Barrière, C., Cerqueira, A., Hunt, S., Tardy, C., Newton, K., Cáceres, J. F., Dubus, P., Malumbres, M. and Barbacid, M. (2007). Cdk1 is sufficient to drive the mammalian cell cycle. *Nature* **448**, 811-815.

Development (2014) 141, 3388-3398 doi:10.1242/dev.106005

Shang, F., Gong, X., McAvoy, J. W., Chamberlain, C., Nowell, T. R., Jr and Taylor, A. (1999). Ubiquitin-dependent pathway is up-regulated in differentiating lens cells. *Exp. Eye Res.* **68**, 179-192.

Sherr, C. J. and Roberts, J. M. (1999). CDK inhibitors: positive and negative regulators of G1-phase progression. *Genes Dev.* **13**, 1501-1512.

Shiokawa, D. and Tanuma, S.-I. (1999). DLAD, a novel mammalian divalent cation-independent endonuclease with homology to DNase II. *Nucleic Acids Res.* **27**, 4083-4089.

Tommasi, S. and Pfeifer, G. P. (1995). In vivo structure of the human cdc2 promoter: release of a p130-E2F-4 complex from sequences immediately upstream of the transcription initiation site coincides with induction of cdc2 expression. *Mol. Cell. Biol.* **15**, 6901-6913.

Vrensen, G. F. J. M., Graw, J. and De Wolf, A. (1991). Nuclear breakdown during terminal differentiation of primary lens fibres in mice: a transmission electron microscopic study. *Exp. Eye Res.* **52**, 647-659.

Vrensen, G. F. J. M., van Marle, J., Jonges, R., Voorhout, W., Breipohl, W. and Wegener, A. R. (2004). Tryptophan deficiency arrests chromatin breakdown in secondary lens fibers of rats. *Exp. Eye Res.* **78**, 661-672.

Wang, W.-L., Li, Q., Xu, J. and Cvekl, A. (2010). Lens fiber cell differentiation and denucleation are disrupted through expression of the N-terminal nuclear receptor box of NCOA6 and result in p53-dependent and p53-independent apoptosis. *Mol. Biol. Cell* **21**, 2453-2468.

Wride, M. A. (2011). Lens fibre cell differentiation and organelle loss: many paths lead to clarity. *Philos. Trans. R. Soc. Lond. B Biol. Sci.* **366**, 1219-1233.

Xie, L., Chen, H., Overbeek, P. A. and Reneker, L. W. (2007). Elevated insulin signaling disrupts the growth and differentiation pattern of the mouse lens. *Mol. Vis.* **13**, 397-407.

Zhang, P., Liégeois, N. J., Wong, C., Finegold, M., Hou, H., Thompson, J. C., Silverman, A., Harper, J. W., DePinho, R. A. and Elledge, S. J. (1997). Altered cell differentiation and proliferation in mice lacking p57KIP2 indicates a role in Beckwith-Wiedemann syndrome. *Nature* **387**, 151-158.

Zhang, P., Wong, C., DePinho, R. A., Harper, J. W. and Elledge, S. J. (1998). Cooperation between the Cdk inhibitors p27(KIP1) and p57(KIP2) in the control of tissue growth and development. *Genes Dev.* **12**, 3162-3167.

Zhao, H., Yang, Y., Rizo, C. M., Overbeek, P. A. and Robinson, M. L. (2004). Insertion of a Pax6 consensus binding site into the alphaA-crystallin promoter acts as a lens epithelial cell enhancer in transgenic mice. *Invest. Ophthalmol. Vis. Sci.* **45**, 1930-1939.

Zheng, Z., Wan, Q., Meixiong, G. and Du, Q. (2014). Cell cycle-regulated membrane binding of NuMA contributes to efficient anaphase chromosome separation. *Mol. Biol. Cell* **25**, 606-619.

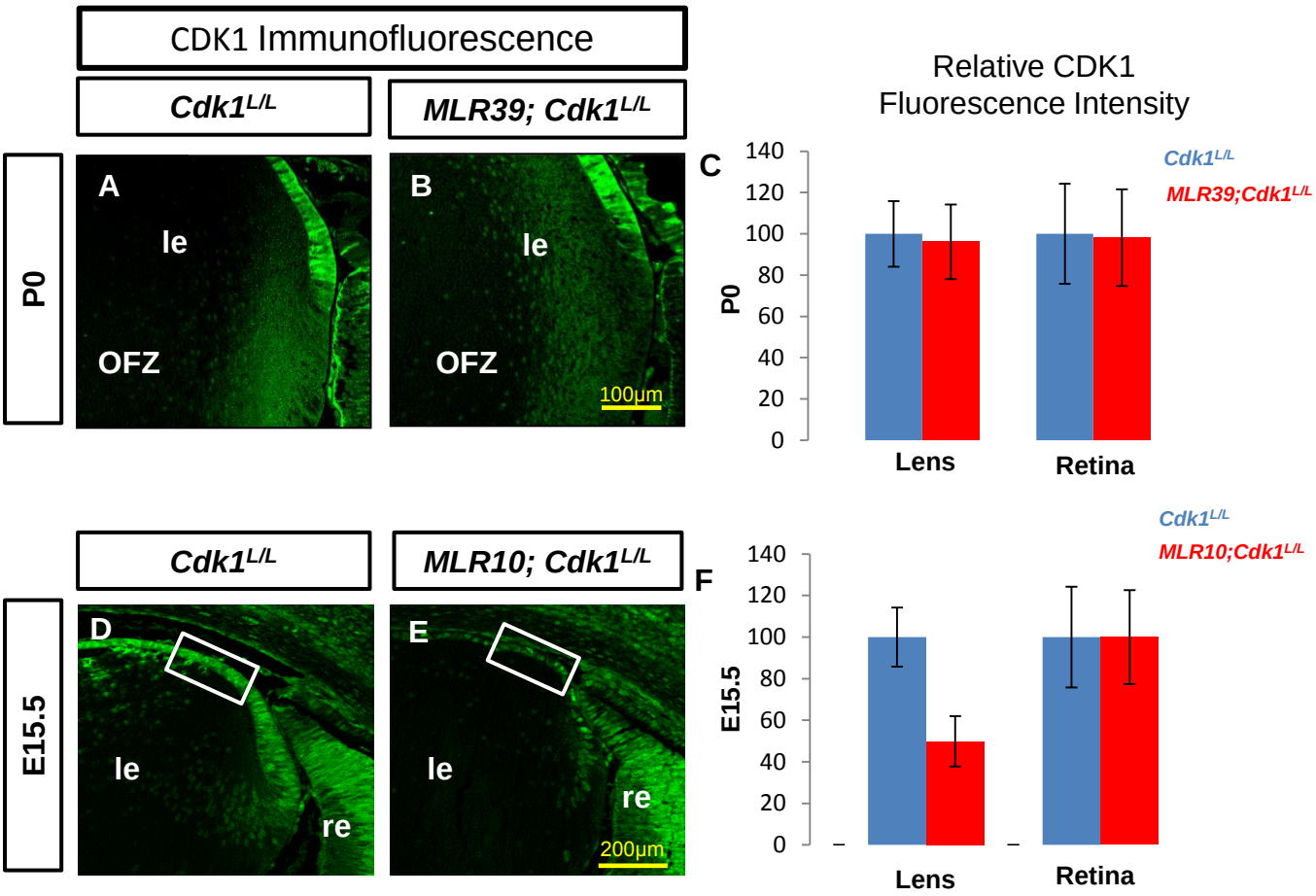

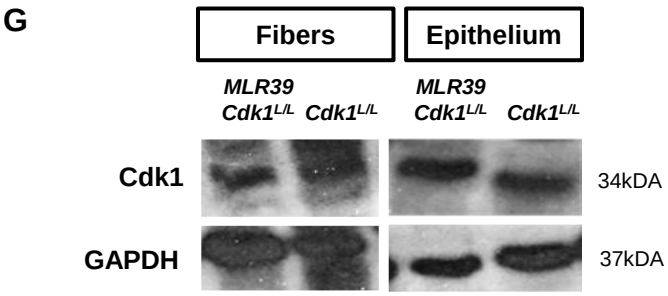

Supplemental Figure 1

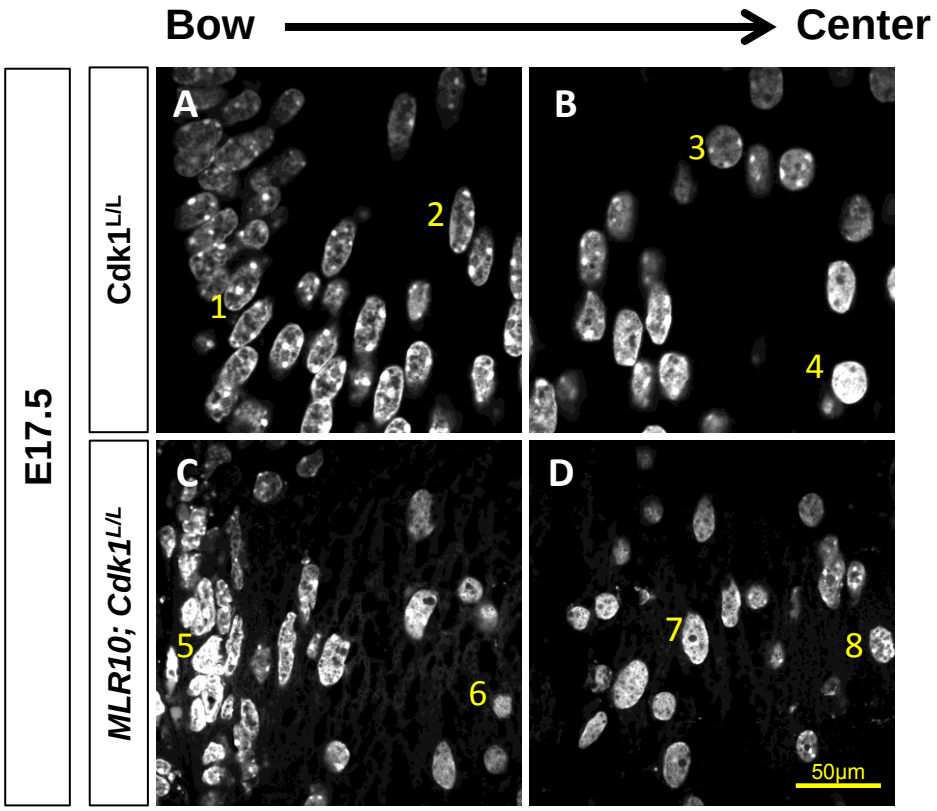

Supplemental Figure 2

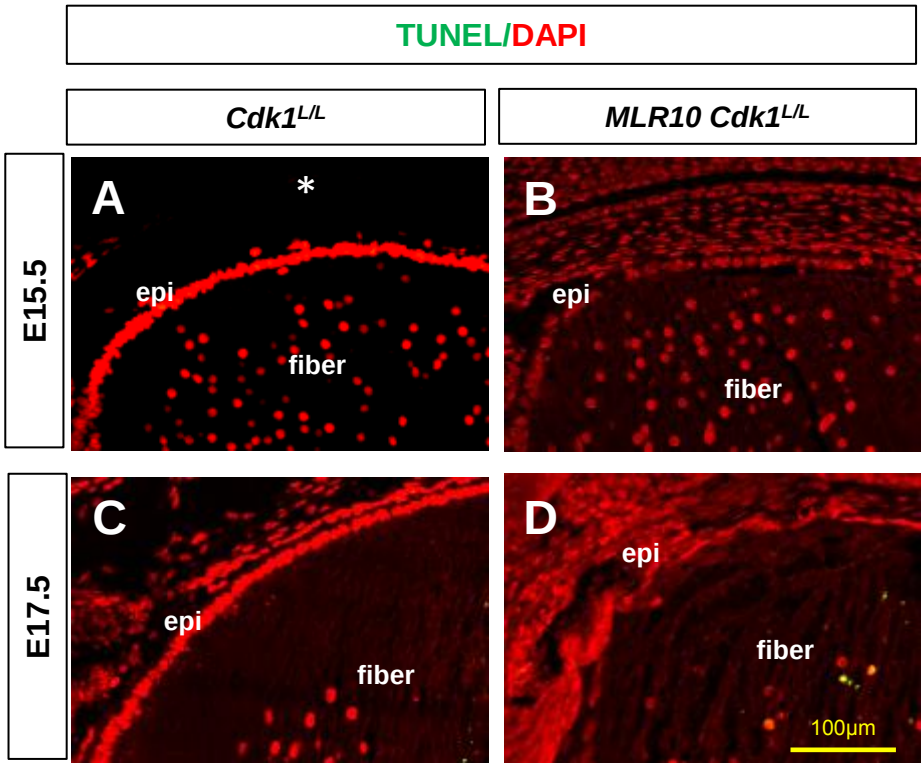

Supplemental Figure 3

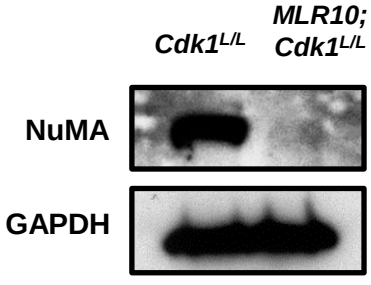

Supplemental Figure 4

Supplemental Figure Legends

Supp. Fig. 1

Cdk1$^{L/L}$ and *MLR39; Cdk1*$^{L/L}$ lenses were compared at P0 (birth) for CDK1 expression (A-C). CDK1 protein is evident in the lens epithelium and nuclei of fiber cells in *Cdk1*$^{L/L}$ lenses (A). The *MLR39* transgene did not reduce immunologically detectable CDK1 expression in the fiber cells of *MLR39; Cdk1*$^{L/L}$ mice (B, C). Western blot analysis supported the immunoflourescent data, as MLR39; Cdk1$^{L/L}$ lenses retained CDK1 protein in the fiber cell mass (G). *Cdk1*$^{L/L}$ and *MLR10; Cdk1*$^{L/L}$ lenses were compared at E15.5 for the expression of CDK1 (D-F). At E15.5 CDK1 was detected throughout the entire epithelium of *Cdk1*$^{L/L}$ lenses and in early differentiating fiber cell nuclei (D); whereas *MLR10; Cdk1*$^{L/L}$ lenses showed a mosaic pattern of CDK1 expression in the epithelium and almost no detectable CDK1 in the fiber cells (E). The fluorescent intensity for immunological detection of CDK1 was reduced 50% in *MLR10; Cdk*$^{L/L}$ lenses relative to the lenses of the of Cre negative controls lenses (F). However, the relative fluorescent intensity of CDK1 detection in the retina did not differ significantly between either the *MLR39; Cdk1*$^{L/L}$, and *Cdk1*$^{L/L}$ mice (C) or the *MLR10 Cdk1*$^{L/L}$ and *Cdk1*$^{L/L}$ mice (F). Relative fluorescent intensity of CDK1 in *MLR39; Cdk1*$^{L/L}$, and *MLR10; Cdk1*$^{L/L}$ lens and retina were measured by ImageJ software and normalized to the control lens and retina (C, F). Scale bars represent 100μm in A and B; 200μm in C-F.

Supp. Fig. 2

DAPI staining was implemented for nuclear structure analysis of *Cdk*$^{L/L}$ (A, B) and *MLR10; Cdk1*$^{L/L}$ (C, D) E17.5 lenses. Consistent nuclear structure changes occur moving inwardly from the lens bow (A) towards the lens center (B) in *Cdk1*$^{L/L}$ lenses. At the lens

bow, control lens nuclei are oval in shape and exhibit intense DAPI foci (A, nucleus 1 and 2). Moving towards the lens center, nuclei become spherical (B, nucleus 3), and contain an intense, even DAPI stain throughout the nucleus (B nucleus 4). *MLR10; Cdk1*$^{L/L}$ lenses do not exhibit consistent nuclear changes. Some nuclei near the bow region exhibit an intense DAPI stain throughout the nucleus, as if it were about to denucleate (C, nucleus 5), whereas some nuclei near the lens center are enlarged and oval shaped (D, nucleus 7 and 8).

Supp. Fig. 3 TUNEL analysis was implemented on E15.5 (A, B) and E17.5 (C, D) *Cdk1*$^{L/L}$ (A, C) and *MLR10; Cdk1*$^{L/L}$ (B, D) lenses to determine if increased apoptosis led to the reduction in epithelial cell number observed in *MLR10; Cdk1*$^{L/L}$ lenses. At E15.5 neither *Cdk1*$^{L/L}$ (A) or *MLR10; Cdk1*$^{L/L}$ (B) exhibited many TUNEL positive nuclei (green) in the epithelial cell layer, despite E15.5 *MLR10; Cdk1*$^{L/L}$ lenses already exhibiting noticeably fewer nuclei in the epithelial cell layer as indicated by the nuclear stain DAPI (red). Although the lens center of *Cdk1*$^{L/L}$ displayed numerous TUNEL positive foci by E17.5, the epithelial cell layer of both E17.5 *Cdk1*$^{L/L}$ (C) and *MLR10; Cdk1*$^{L/L}$ (D) lacked any detectable TUNEL positive signal. Sections were counterstained with DAPI (red) in A-D. Scale bar represents 100 μm in A-D.

Supp. Fig. 4

Western blot analysis using an antibody to NuMA revealed a reduction in total NuMA levels at E18.5 in *MLR10; Cdk1*$^{L/L}$ lenses (right lane) relative to the *Cdk1*$^{L/L}$ lenses (left lane). Anti-GAPDH was used as a loading control.